Current Control Method with Control Inputs in Polar Coordinates for SPMSM Based on Linearized Model

Takayuki Miyajima and Hiroshi Fujimoto
The University of Tokyo
Kashiwa, Chiba, Japan

Masami Fujitsuna
DENSO CORPORATION
Kariya, Aichi, Japan

***Abstract*—SPMSMs (Surface Permanent Magnet Synchronous Motors) are employed for many industrial applications. For quick torque response under voltage limit, voltage phase control method had been proposed. However, it needs to switch the mode of controller. This paper proposes a flux-weakening control method for SPMSM using control inputs in polar coordinates to reduce the number of mode transition. This control method is designed with a precise plant model. In addition, the authors investigate controller design using control inputs in polar coordinates instead of d-axis and q-axis voltage within voltage limit.**

I. Introduction

PMSMs (Permanent Magnet Synchronous Motors) are widely employed in many industries because of high efficiency and high power density. In particular, SPMSMs are used for machine tool and electric power steering system. PMSM drive systems use flux-weakening control for the wide operating range but quick current response is difficult because of voltage amplitude limitation.

Quick flux-weakening control methods had been proposed. The modulation feedback methods [1], [2] modified d-axis current reference so that d-axis and q-axis voltage references are within voltage limit. However, modulation feedback method cannot achieve quick torque response because the modulation feedback loop is the outer of the current feedback loop which has low bandwidth due to voltage saturation. Ref. [3] proposed dead-beat control which considers voltage limit and current limit. The dead-beat control method makes tracking error if the modeling error exists. The voltage phase control method [4]–[6] operates voltage phase directly to compensate torque tracking error. It has no inner loop. Therefore, the authors consider that the voltage phase control method is suitable for flux-weakening region.

In the previous paper, the authors proposed a precise model-based design method of voltage phase controller by using a linearized plant model and quick torque response was achieved [7], [8]. However, the voltage phase control method must switch the mode of the controller. The mode transition deteriorates torque response.

In order to reduce the number of mode transition, this paper proposes a flux-weakening control method using control inputs in polar coordinates for SPMSM. In order to suppress flux-strengthen operation, the proposed control method starts to controls d-axis current by voltage amplitude when the operating point transits from flux-weakening range to linear region. On the other hand, in flux-weakening range, it operates voltage phase only and stops the integration of d-axis current controller. Therefore, proposed control method achieves transition between flux-weakening region and linear region automatically. This control system is designed based on a linearized plant model. Simulation and experimental results are performed to show the advantages of the proposed method.

Moreover, in linear region, control methods using voltage amplitude and voltage phase as control inputs instead of d-axis and q-axis voltages were proposed [9]–[11]. However, controller design method had not been discussed precisely. This paper investigates a model-based design method with control inputs in polar coordinates within voltage limit and discusses the controllability.

II. Model and Linearzation

A. dq Model of SPMSM

The voltage equation of SPMSM in dq axis is represented by

$$\begin{aligned}\frac{\mathrm{d}}{\mathrm{d}t}\boldsymbol{x} &= \begin{bmatrix} -\frac{R}{L} & \omega_e \\ -\omega_e & -\frac{R}{L} \end{bmatrix}\boldsymbol{x} + \frac{1}{L}\begin{bmatrix} v_d(\boldsymbol{u}) \\ v_q(\boldsymbol{u}) - \omega_e K_e \end{bmatrix} \\ &= \boldsymbol{f}(\boldsymbol{x},\ \boldsymbol{u}), \qquad (1)\\ v_d(\boldsymbol{u}) &= -V_a \sin\delta, \quad v_q(\boldsymbol{u}) := V_a\cos\delta, \\ \boldsymbol{x} &:= [i_d \quad i_q]^{\mathrm{T}}, \quad \boldsymbol{u} = [V_a \quad \delta]^{\mathrm{T}},\end{aligned}$$

where i_d, i_q are the d-axis and q-axis current, R is the stator winding resistance, L is the inductance, ω_e is the electric angular velocity, and K_e is the back EMF constant, V_a is the voltage amplitude, and δ is the voltage phase.

B. Linearized dq Model

In flux-weakening region, the voltage amplitude is saturated and the manipulated variable is the voltage phase only. Therefore, (1) is not suitable for controller design. For model-based design, (1) is linearized around an equilibrium point which satisfies $\boldsymbol{f}(\boldsymbol{x}_o,\ \boldsymbol{u}_o) = 0$ as follows:

$$\begin{aligned}&\frac{\mathrm{d}}{\mathrm{d}t}\Delta\boldsymbol{x} = \Delta\boldsymbol{A}\Delta\boldsymbol{x} + \Delta\boldsymbol{B}\Delta\boldsymbol{u}, \qquad (2)\\ &\Delta\boldsymbol{A} := \left[\frac{\partial\boldsymbol{f}(\boldsymbol{x}_o,\ \boldsymbol{u}_o)}{\partial\boldsymbol{x}}\right]^{\mathrm{T}} = \begin{bmatrix} -\frac{R}{L} & \omega_e \\ -\omega_e & -\frac{R}{L} \end{bmatrix}, \\ &\Delta\boldsymbol{B} := \left[\frac{\partial\boldsymbol{f}(\boldsymbol{x}_o,\ \boldsymbol{u}_o)}{\partial\boldsymbol{u}}\right]^{\mathrm{T}} = \begin{bmatrix} -\frac{1}{L}\sin\delta_o & -\frac{V_{ao}}{L}\cos\delta_o \\ \frac{1}{L}\cos\delta_o & -\frac{V_{ao}}{L}\sin\delta_o \end{bmatrix}, \\ &\Delta\boldsymbol{x} = \boldsymbol{x} - \boldsymbol{x}_o,\ \Delta\boldsymbol{x} := [\Delta i_d\ \Delta i_q]^{\mathrm{T}},\ \boldsymbol{x}_o = [i_{do}\ i_{qo}]^{\mathrm{T}}, \\ &\Delta\boldsymbol{u} = \boldsymbol{u} - \boldsymbol{u}_o,\ \Delta\boldsymbol{u} := [\Delta V_a\ \Delta\delta]^{\mathrm{T}},\ \boldsymbol{u}_o = [V_{ao}\ \delta_o]^{\mathrm{T}}.\end{aligned}$$

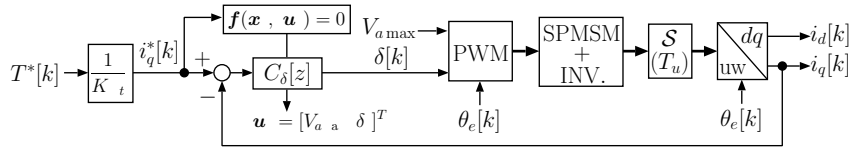

(a) Voltage phase control only (conventional method)

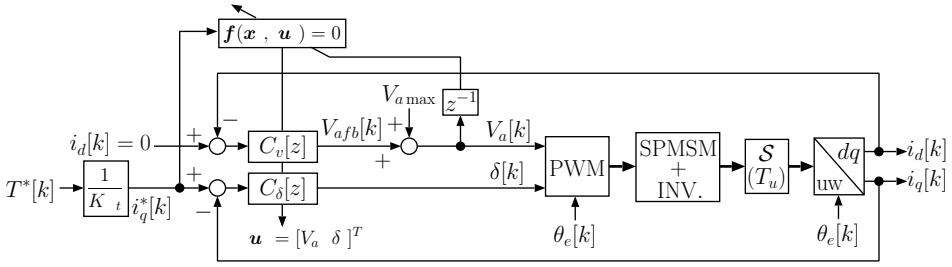

(b) Voltage phase control with voltage amplitude control (proposed method)

Fig. 1. Flux-weakening control with voltage phase control

This equilibrium point is an operating point on steady-state.

The transfer functions from $\Delta\boldsymbol{u}$ to $\Delta\boldsymbol{x}$ are expressed by

$$\begin{bmatrix} \Delta i_d \\ \Delta i_q \end{bmatrix} = \begin{bmatrix} \Delta P_{11}(s) & \Delta P_{12}(s) \\ \Delta P_{21}(s) & \Delta P_{22}(s) \end{bmatrix} \begin{bmatrix} \Delta V_a \\ \Delta\delta \end{bmatrix}, \tag{3}$$

$$\Delta P_{11}(s) = \frac{-\frac{1}{L}\sin\delta_o\left\{s+\frac{R}{L}-\omega_e\tan\left(\frac{\pi}{2}-\delta_o\right)\right\}}{s^2+2\frac{R}{L}s+\frac{R^2}{L^2}+\omega_e^2}, \tag{4}$$

$$\Delta P_{12}(s) = \frac{-\frac{V_{ao}}{L}\cos\delta_o\left(s+\frac{R}{L}+\omega_e\tan\delta_o\right)}{s^2+2\frac{R}{L}s+\frac{R^2}{L^2}+\omega_e^2}, \tag{5}$$

$$\Delta P_{21}(s) = \frac{\frac{1}{L}\cos\delta_o\left(s+\frac{R}{L}+\omega_e\tan\delta_o\right)}{s^2+2\frac{R}{L}s+\frac{R^2}{L^2}+\omega_e^2}, \tag{6}$$

$$\Delta P_{22}(s) = \frac{-\frac{V_{ao}}{L}\sin\delta_o\left\{s+\frac{R}{L}-\omega_e\tan\left(\frac{\pi}{2}-\delta_o\right)\right\}}{s^2+2\frac{R}{L}s+\frac{R^2}{L^2}+\omega_e^2}. \tag{7}$$

Our previous paper proposed a precise model-based voltage phase controller which is designed with $\Delta P_{22}(s)$ [7]. In this paper, a voltage amplitude controller which controls d-axis current is designed by utilizing $\Delta P_{11}(s)$.

III. FLUX-WEAKENING CONTROL USING CONTROL INPUTS IN POLAR COORDINATES

In this section, proposed flux-weakening control system using control inputs in polar coordinates is designed and compared with conventional voltage phase control method. The block diagrams of conventional method and proposed method are described in Fig. 1(a) and 1(b), respectively. Conventional method operates the voltage phase only. On the other hand, proposed method utilizes the voltage amplitude in addition to the voltage phase.

A. Conventional Method [7]

The voltage phase controller $C_\delta[z]$ is designed with a precise plant model $\Delta P_{22}(s)$ which is described in (7). However, this plant model is small signal model. Hence, an equilibrium point $\boldsymbol{u}_o$ is essential to controller design.

TABLE I. PARAMETERS UNDE THE TEST

inductance L	0.185 mH
stator winding resistance R	33.7 Ω
number of pole pairs P	7
back EMF constant K_e	11.60 mV/(rad/s)
dc-bus voltage of three-phase inverter V_{dc}	12 V
maximum modulation index $M_{\max}$	1.0
control period T_u	0.1 ms

On steady-state, the average q-axis current $\bar{i}_q$ is represented by

$$\bar{i}_q = \frac{\bar{V}_a}{\sqrt{R^2+\omega_e^2L^2}}\sin\left(\bar{\delta}+\tan^{-1}\frac{R}{\omega_eL}\right)-\frac{\omega_eK_eR}{R^2+\omega_e^2L^2}, \tag{8}$$

where $\bar{V}_a$ is the average voltage amplitude and $\bar{\delta}$ is the average voltage phase. By solving (8) for $\bar{\delta}$, the average voltage phase $\bar{\delta}$ is given by

$$\bar{\delta} = \sin^{-1}\left\{\frac{\left(R^2+\omega_e^2L^2\right)\bar{i}_q+\omega_eK_eR}{\sqrt{R^2+\omega_e^2L^2}\bar{V}_a}\right\}-\tan^{-1}\frac{R}{\omega_eL}. \tag{9}$$

In flux-weakening region, the voltage amplitude is fixed as maximum value $V_{a\max}$. Thus, $\bar{\delta}$ can be calculated by obtaining q-axis current. For controller design, q-axis current reference is selected as $\bar{i}_q$ and an equilibrium point can be defined as $\boldsymbol{u}_o := [V_{a\max}\ \ \bar{\delta}]^{\mathrm{T}}$ from (9).

The closed-loop characteristic equation of voltage phase control at the defined equilibrium point is expressed by

$$1+\Delta P_{22}(s)C_\delta(s)=0. \tag{10}$$

In order to set all closed-loop poles at arbitrary values, a PID controller is selected as the voltage phase controller $C_\delta(s)$. $C_\delta(s)$ is designed by pole-placement method. The discretized controller $C_\delta[z]$ is obtained by Tustin transformation with the control period T_u.

B. Proposed Method

The voltage phase controller $C_\delta[z]$ is the same with that of conventional method.

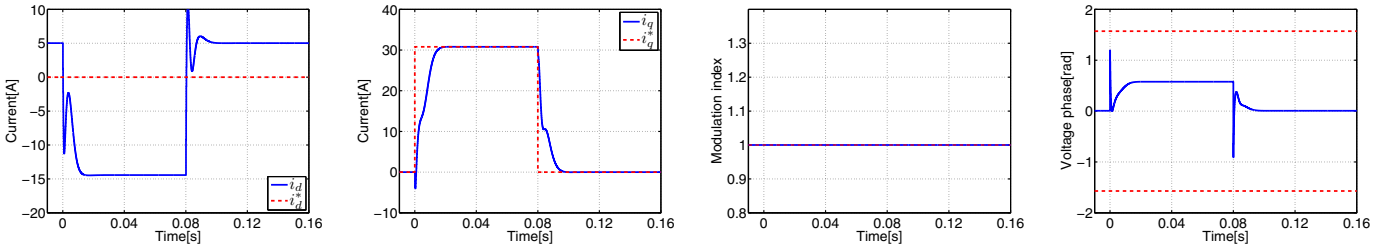

(a) d-axis current i_d (b) q-axis current i_q (c) Modulation index (d) Voltage phase δ

Fig. 2. Simulation result in flux-weakening region (conventional method, 800 rpm).

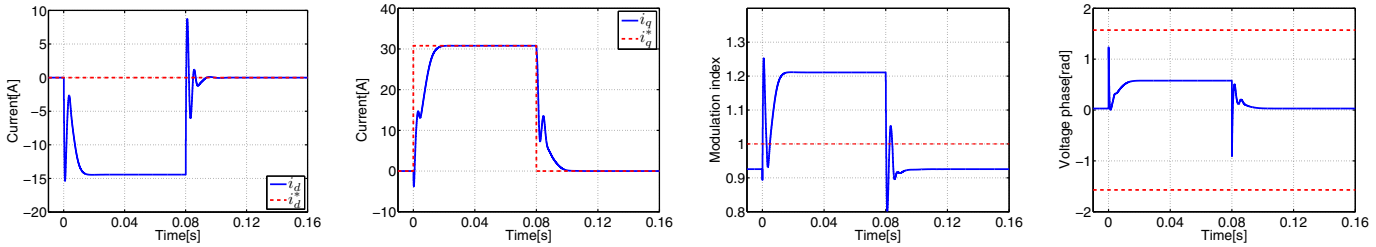

(a) d-axis current i_d (b) q-axis current i_q (c) Modulation index (d) Voltage phase δ

Fig. 3. Simulation result in flux-weakening region (proposed method, 800 rpm).

The voltage amplitude controller $C_v[z]$ controls d-axis current by using voltage amplitude V_a to prevent flux-strengthening operation. Thus, it is designed with $\Delta P_{11}(s)$. The closed-loop characteristic equation of voltage amplitude control at an equilibrium point is expressed by

$$1 + \Delta P_{11}(s) C_v(s) = 0. \tag{11}$$

The voltage amplitude controller which is a PID controller is designed by pole-placement method to place all closed-loop poles at arbitrary values. If the voltage amplitude is saturated, the state variables of the voltage amplitude controller is not renewed (anti-windup control).

In proposed method, the voltage amplitude is not fixed. Therefore, the controller output $V_a[k-1]$ delayed one sample is used as an equilibrium point V_{ao}. δ_o is calculated from (9).

Proposed method can reduce the number of mode transition. However, it cannot apply in all operating region. The controllability of proposed method is discussed in the next section.

C. Simulation and Experiment

The effectiveness of the proposed method is verified from simulation and experimental results. Table I shows the parameters under the test.

The plant poles p_1 and p_2 are expressed by

$$p_1,\ p_2 = -\frac{R}{L} \pm j\omega_e. \tag{12}$$

In high-speed region, the plant has fast complex conjugate poles. All closed-loop poles should be faster than the plant poles. Therefore, at the high-speed region, the proposed method places all closed-loop poles on a circle which goes through the plant poles and has a center at the origin. In both conventional method and proposed method, the real parts of all close-loop poles of voltage phase controller are placed at -600 rad/s. In order to place a high priority on q-axis current tracking, the real parts of all voltage amplitude control loop poles are set at -300 rad/s.

Fig. 2 and 3 show simulation results at 800 rpm of conventional method and proposed method, respectively. The dotted lines in Fig. 2(c) and 3(c) are described the maximum modulation index $M_{\max}$. In simulation and experiment, the controller switch structure is not used.

By using our previous proposed design method, conventional method controls q-axis current quickly. However, it manipulates voltage phase only. Therefore, as shown Fig. 2(a), flux-strengthening operation ($i_d > 0$) is caused. In order to suppress flux-strengthening operation, conventional method needs to switch the mode of controller. On the other hand, proposed method suppresses flux-strengthening operation by the voltage amplitude controller without mode transition as shown Fig. 3(a). Under the voltage amplitude saturation, the voltage amplitude does not diverge by anti-windup control. In addition, proposed method prioritizes q-axis current control. Therefore, q-axis current response of proposed method is the same with that of conventional method. The effectiveness of proposed method is verified.

Experiments were conducted under the same condition as simulations. Experimental results of conventional method and proposed method are reported in Fig. 4 and Fig. 5, respectively. Conventional method achieves quick q-axis current response but it causes flux-strengthening operation ($i_d > 0$). On the other hand, proposed method makes transition between flux-weakening region and linear region automatically. The effectiveness of proposed method is verified.

IV. CURRENT CONTROL USING CONTROL INPUTS IN POLAR COORDINATES IN LINEAR REGION

In this section, the controllability and design method for current control method using control inputs in polar coordi-

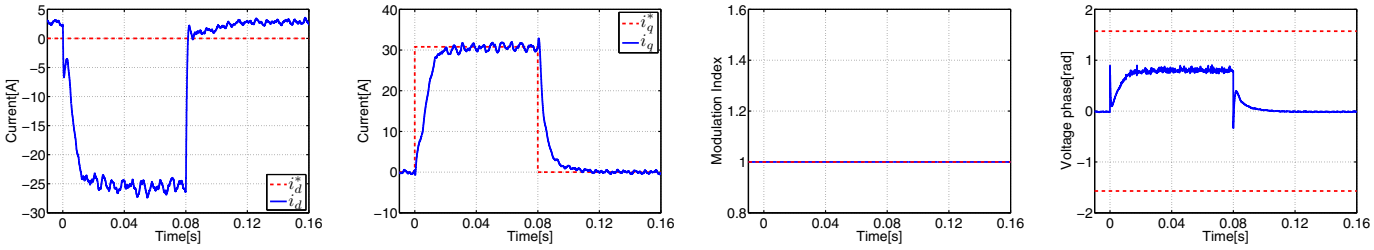

(a) d-axis current i_d (b) q-axis current i_q (c) Modulation index (d) Voltage phase δ

Fig. 4. Experimental result in flux-weakening region (conventional method, 800 rpm).

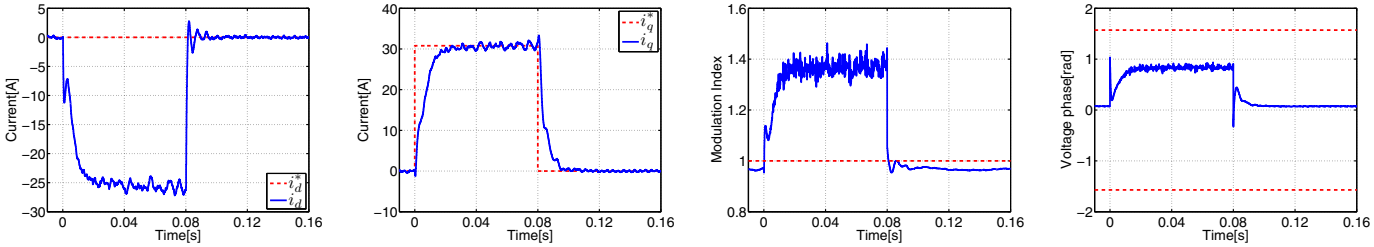

(a) d-axis current i_d (b) q-axis current i_q (c) Modulation index (d) Voltage phase δ

Fig. 5. Experimental result in flux-weakening region (proposed method, 800 rpm).

nates in linear region are investigated.

A. Analysis of Controllability

The controllability is analyzed with the controllability matrix as shown (13).

$$\boldsymbol{U}_c = \Delta\boldsymbol{B} = \begin{bmatrix} -\frac{1}{L}\sin\delta_o & -\frac{V_{ao}}{L}\cos\delta_o \\ \frac{1}{L}\cos\delta_o & -\frac{V_{ao}}{L}\sin\delta_o \end{bmatrix} \tag{13}$$

The voltage phase control system controls the q-axis current (torque) with the voltage phase. From (13), as $V_{ao} = 0$, rank $\boldsymbol{U}_c \neq 2$. Therefore, the voltage phase control system cannot change q-axis current from zero q-axis current at zero speed. Although the proposed control method can reduce the number of mode transition, it needs a controller switching structure and cannot be applied in all operating range.

Here, a control system which controls the q-axis and d-axis currents by the voltage amplitude and the voltage phase respectively is assumed. This system cannot vary d-axis current if $V_{ao} = 0$ at zero speed. However, when $V_{ao} = 0$ at zero speed, $i_d = 0$ is desired in linear region for SPMSM. Therefore, this system can apply in all operating range but it needs optimal d-axis current reference in flux-weakening region. Next, a model-based design of this control system is investigated.

B. Control System Design

1) Linearization and Approximation: For basic consideration, it is assumed that an operating point is in linear region. In linear region, the decoupling control can be applied. The amplitude and phase of decoupling control input are expressed by

$$V_{ad}(i_d,\ i_q) = \omega_e\sqrt{L^2 i_q^2 + (Li_d + K_e)^2}, \tag{14}$$

$$\delta_d(i_d,\ i_q) = \tan^{-1}\frac{\omega_e L i_q}{\omega_e L i_d + K_e}. \tag{15}$$

This system controls the q-axis and d-axis currents by the voltage amplitude and the voltage phase, respectively. Therefore, the voltage amplitude and the voltage phase are given by

$$V_a = V_{ad} + V_{afb}, \quad \delta = \delta_d + \delta_{fb}, \tag{16}$$

where V_{afb} is the q-axis current controller output and δ_{fb} is the d-axis current controller output.

(1) and (16) are linearized around equilibrium point. The linearized plant model is represented by

$$\frac{\mathrm{d}}{\mathrm{d}t}\begin{bmatrix}\Delta i_d \\ \Delta i_q\end{bmatrix} = \Delta\boldsymbol{A}\begin{bmatrix}\Delta i_d \\ \Delta i_q\end{bmatrix} + \Delta\boldsymbol{B}\begin{bmatrix}\Delta V_{afb} \\ \Delta\delta_{fb}\end{bmatrix}. \tag{17}$$

Though the decoupling control is applied, the coupling term exists due to the coupling between the voltage amplitude and the voltage phase. Here, it is assumed that an operating point is in low speed region and (17) can be approximated as follows:

$$\frac{\mathrm{d}}{\mathrm{d}t}\begin{bmatrix}\Delta i_d \\ \Delta i_q\end{bmatrix} \simeq -\frac{R}{L}\begin{bmatrix}1 & 0 \\ 0 & 1\end{bmatrix}\begin{bmatrix}\Delta i_d \\ \Delta i_q\end{bmatrix} + \boldsymbol{B}\begin{bmatrix}\Delta V_{afb} \\ \Delta\delta_{fb}\end{bmatrix}. \tag{18}$$

From (18), the transfer functions are given by

$$\begin{bmatrix}\Delta i_d \\ \Delta i_q\end{bmatrix} = \begin{bmatrix}\Delta P_{l11}(s) & \Delta P_{l12}(s) \\ \Delta P_{l21}(s) & \Delta P_{l22}(s)\end{bmatrix}\begin{bmatrix}\Delta V_{afb} \\ \Delta\delta_{fb}\end{bmatrix}, \tag{19}$$

$$\Delta P_{l11}(s) := \frac{-\sin\delta_o}{Ls + R}, \tag{20}$$

$$\Delta P_{l12}(s) := \frac{-V_{ao}\cos\delta_o}{Ls + R}, \tag{21}$$

$$\Delta P_{l21}(s) := \frac{\cos\delta_o}{Ls + R}, \tag{22}$$

$$\Delta P_{l22}(s) := \frac{-V_{ao}\sin\delta_o}{Ls + R}. \tag{23}$$

q-axis current controller and d-axis current controller are designed with $\Delta P_{21}(s)$ and $\Delta P_{12}(s)$, respectively.

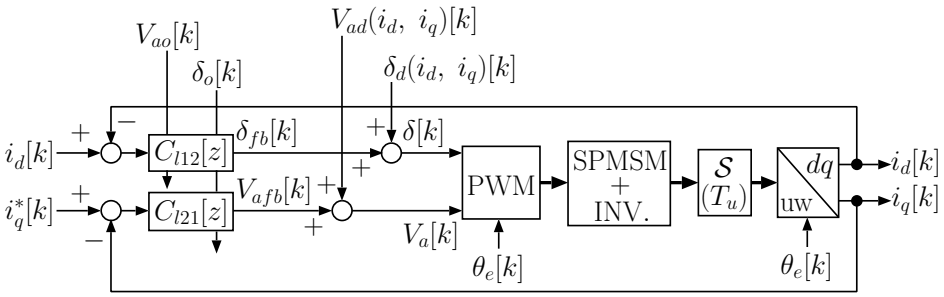

Fig. 6. Block diagram of current control at linear range with control inputs in polar coordinates

2) Controller Design: The block diagram of current control at linear range with control inputs in polar coordinates is illustrated in Fig. 6. In order to place all closed-loop poles at arbitrary values, the q-axis current controller $C_{21}[z]$ and the d-axis current controller $C_{12}[z]$ are PI controllers as shown in (24) and (25), respectively.

$$C_{21}(s) = \frac{K_{P21}s + K_{I21}}{s}. \tag{24}$$

$$C_{12}(s) = \frac{K_{P12}s + K_{I12}}{s}. \tag{25}$$

In order to suppress modeling error caused by approximation and coupling term $\Delta P_{l11}(s)$ and $\Delta P_{l22}(s)$. PI controllers are not designed to be pole-zero cancellation. Coefficient diagram method [12] applies to feedback controller design.

Define the desirable characteristic equations of q-axis current control-loop and d-axis current control-loop as follows:

$$s^2 + a_{1l21}s + a_{0l21} = 0 \tag{26}$$

$$s^2 + a_{1l12}s + a_{0l12} = 0 \tag{27}$$

The q-axis and d-axis current controller gains which achieve the desirable characteristic equations are given by

$$K_{P21} = \frac{a_{1l21}L - R}{\cos\delta_o}, \tag{28}$$

$$K_{I21} = \frac{a_{0l21}L}{\cos\delta_o}, \tag{29}$$

$$K_{P12} = \frac{a_{1l12}L - R}{-V_{ao}\cos\delta_o}, \tag{30}$$

$$K_{I12} = \frac{a_{0l12}L}{-V_{ao}\cos\delta_o}. \tag{31}$$

The coefficients of characteristic equations are selected to be the standard form of coefficient diagram method as follows:

$$\gamma_{1l21} = \frac{a_{1l21}^2}{a_{0l21}} = 2.5, \tag{32}$$

$$\tau_{21} = \frac{a_{1l21}}{a_{0l21}}, \tag{33}$$

$$\gamma_{1l12} = \frac{a_{1l12}^2}{a_{0l12}} = 2.5, \tag{34}$$

$$\tau_{12} = \frac{a_{1l12}}{a_{0l12}}, \tag{35}$$

where τ_{12} and τ_{21} refer the equivalent time constants which determine feedback bandwidth.

From (30) and (31), the d-axis current controller is high gain controller around $V_{ao} = 0$. Thus, the equivalent time constant of d-axis current is varied depending on the operating point to avoid control input saturation. The equivalent time constants are selected as

$$\tau_{21} = 10T_u, \tag{36}$$

$$\tau_{12} = \begin{cases} 10T_u & (|V_{ao}\cos\delta_o| \geq 0.01V_{a\max}) \\ \frac{0.1V_{a\max}}{|V_{ao}\cos\delta_o|}T_u & (\text{otherwise}) \end{cases}. \tag{37}$$

In addition, in order to avoid zero division, V_{ao} and δ_o are limited as $V_{a\max} \geq |V_{ao}| \geq 0.001V_{a\max}$ and $|\delta_o| \leq \frac{0.9\pi}{2}$, respectively.

The equilibrium point of the plant model is obtained form the controller outputs as follows:

$$\delta_o[k] = \delta[k-1] = \delta_{fb}[k-1] + \delta_d[k], \tag{38}$$

$$V_{ao}[k] = V_a[k] = V_{afb}[k] + V_{ad}[k]. \tag{39}$$

The voltage phase on equilibrium point is the controller output delayed one sample. The voltage amplitude on equilibrium point is only used for the design of the d-axis current controller which operates the voltage phase. Therefore, after the q-axis current controller calculation, the real-time voltage amplitude can be utilized for the d-axis current controller design.

C. Simulation and Experiment

The controller design method of a current control with control inputs in polar coordinates is evaluated from simulation and experimental results. The parameters under the test are shown Table I.

Fig. 7 and 8 report simulation results at 0 rpm and 400 rpm, respectively. The dotted lines in Fig. 7(c) and 8(c) show the maximum modulation index $\pm M_{\max}$. The dotted lines in Fig. 7(d) and 8(d) represent the voltage phase limiter ($\pm\delta_{\max} = \pm\frac{\pi}{2}$ rad).

At 0 rpm, the modeling error caused by approximation is not exist and the coupling terms $\Delta P_{l11}(s)$ and $\Delta P_{l22}(s)$ are small. Proposed design method achieves quick d-axis and q-aixs current responses. In coefficient diagram method, closed-loop poles are complex conjugate poles. Therefore, overshoots happen but they are small. Moreover, $V_a \simeq 0$ around 0 Nm. Thus, the controllability is not assured. However, proposed design method makes small gain d-axis current controller when $V_a \simeq 0$ and the controller output (the voltage phase) is stable.

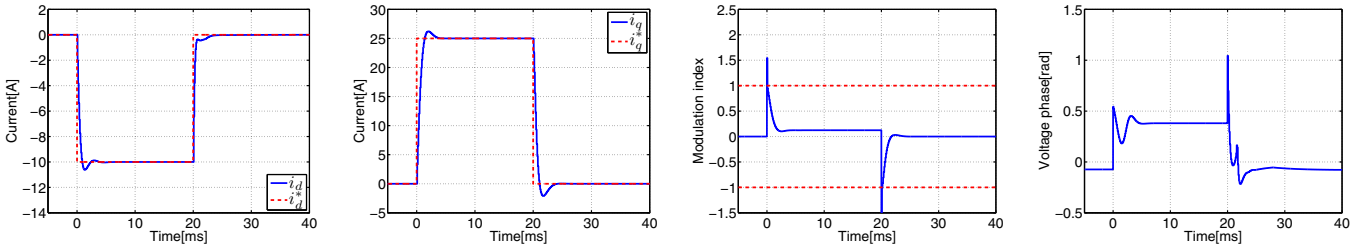

(a) d-axis current i_d (b) q-axis current i_q (c) Modulation index (d) Voltage phase δ

Fig. 7. Simulation result of current control with control inputs in polar coordinates at linear range (0 rpm).

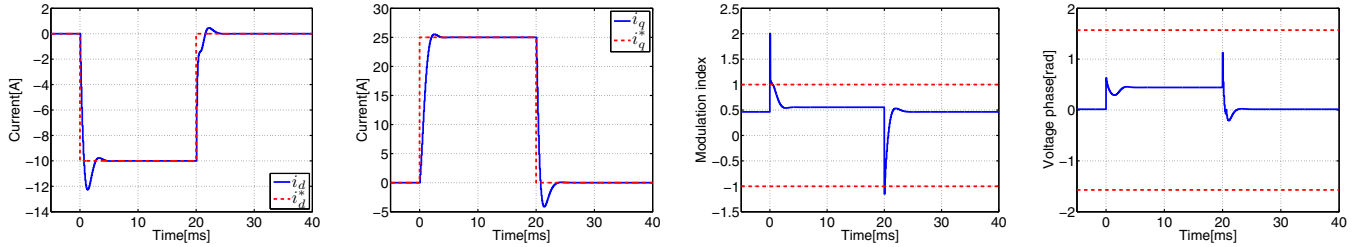

(a) d-axis current i_d (b) q-axis current i_q (c) Modulation index (d) Voltage phase δ

Fig. 8. Simulation result of current control with control inputs in polar coordinates at linear range (400 rpm).

On the other hand, the coupling terms $\Delta P_{l11}(s)$ and $\Delta P_{l22}(s)$ and the modeling error caused by approximation are large at 400 rpm. Although the settling time at 400 rpm is the same as that of simulation results at 0 rpm, the large overshoots happen. In order to suppress these large overshoot, more precise controller design method is needed.

Experimental results at 0 rpm and 400 rpm are illustrated in Fig. 7 and 8, respectively. If $V_{ao} \simeq 0$, the controllability is not assured. Therefore, the d-axis current controller is designed to be small gain around 0 Nm at 0 rpm. However, the voltage phase is oscillated owing to measurement noise. On the other hand, the oscillation of the voltage phase does not occur at 400 rpm because the controllability is assured at this operating point.

From experimental results, around $V_{ao} \simeq 0$, the uncontrollability causes oscillation of the voltage phase. This oscillation could lead to current ripple. Therefore, a technique which reduces the voltage phase oscillation is essential for a current control with control inputs in polar coordinates.

V. CONCLUSION

This paper proposes a flux-weakening control method using control inputs in polar coordinates based on linearized model. The proposed method achieves seamless transfer between linear range and flux-weakening range. Moreover, q-axis current response of the proposed method is quick and the same as that of the conventional method.

In addition, the controllability of control inputs in polar coordinates is analyzed. This analysis shows the voltage phase control system cannot apply in all operating range and a possibility that q-axis and d-axis currents can be controlled by the voltage amplitude and the voltage phase, respectively. In linear range, a current control method using control inputs in polar coordinates is investigated. The realization of this control method is shown by simulation and experimental results. However, the coupling terms which are neglected for basic consideration causes large overshoot and the voltage phase is oscillated at the uncontrollable operating point.

In our future works, a controller switching structure which suppresses torque variation during mode transition is studied. Moreover, a technique which prevents the voltage phase oscillation for a current control with control inputs in polar coordinates within voltage limit will be developed.

REFERENCES

[1] T.-S. Kwon, G.-Y. Choi, M.-S. Kwak, and S.-K Sul, "Novel Flux-Weakening Control of an IPMSM for Quasi-Six-Step Operation", IEEE Trans. Ind. Appl., Vol. 44, NO. 6, pp. 1722–1723, 2008.

[2] H. Liu, Z. Q. Zhu, E. Mohamed, Y. Fu, and X. Qi, "Flux-Weakening Control of Nonsalient Pole PMSM Having Large Winding Inductance, Accounting for Resistive Voltage Drop and Inverter Nonlinearities", IEEE Trans. Power Electronics, Vol. 27, No. 2, pp. 942–952, 2012.

[3] C.-H. Choi, J.-K. Seok, and R. D. Lorenz, "Wide-Speed Direct Torque and Flux Control for Interior PM Synchronous Motors Operating at Voltage and Current Limits", The 2011 IEEE Energy Conversion Congress and Exposition, pp.371–376, 2011.

[4] H. Nakai, H. Ohtani, E. Satoh, and Y. Inaguma: "Development and Testing of the Torque Control for the Permanent-Magnet Synchronous Motor", IEEE Trans. Ind. Electron., Vol. 52, No. 3, pp. 800–806, 2005.

[5] W. Hatsuse, Y. Notohara, K. Ohi, K. Tobari, K. Tamura, C. Unoko, and Y. Iwaji, "A Stable Field-Weakening Control Using Voltage Phase Operations in the High-Power Region", The 2010 International Power Electronics Conference, pp.599–604, 2010.

[6] K. Kondo and S. Kitamura, "Torque Control Method for Permanent Magnet Synchronous Motor Operating in Field Weakening Region at Middle Speed Range", IEEJ Journal of Industry Applications, Vol. 2, No. 2, pp. 106–112, 2013.

[7] T. Miyajima, H. Fujimoto, and M. Fujitsuna, "Model-based Design of Voltage Phase Controller for SPMSM in Field-weakening Region", 28th Annual Applied Power Electronics Conference and Exposition, pp.2266–2272, 2013.

[8] T. Miyajima, H. Fujimoto, and M. Fujitsuna, "Model-based Voltage Phase Control for IPMSM with Equilibrium Point Search", 15th European Conference on Power Electronics and Applications, 2013.

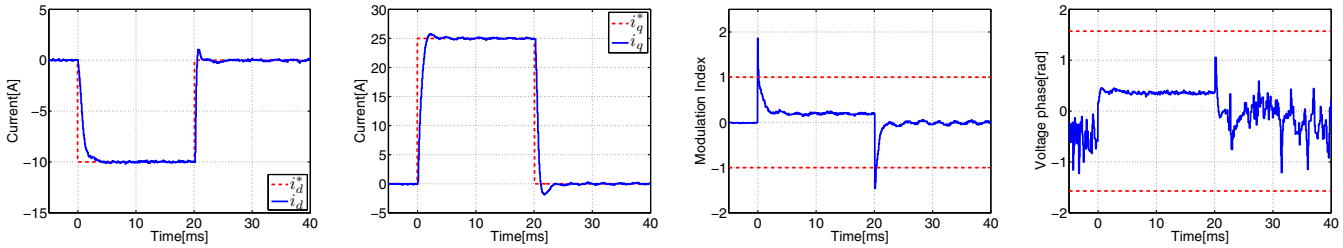

(a) d-axis current i_d (b) q-axis current i_q (c) Modulation index (d) Voltage phase δ

Fig. 9. Experimental result of current control with control inputs in polar coordinates at linear range (0 rpm).

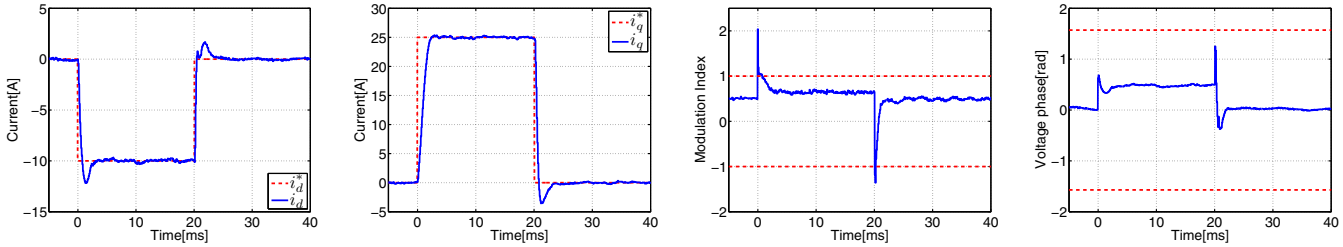

(a) d-axis current i_d (b) q-axis current i_q (c) Modulation index (d) Voltage phase δ

Fig. 10. Experimental result of current control with control inputs in polar coordinates at linear range (400 rpm).

[9] L. Tang, L. Zhong, M. F. Rahman, and Y. Hu, "A Novel Direct Torque Controlled Interior Permanent Magnet Synchronous Machine Drive With Low Ripple in Flux and Torque and Fixed Switching Frequency", IEEE Trans. Power Electronics, Vol. 19, No. 2, pp. 346–354, 2004.

[10] Y. Inoue, S. Motrimoto, and S. Morimoto, "Examination and Linearization of Torque Control System for Direct Torque Controlled IPMSM", IEEE Trans. Ind. Appl., Vol. 46, No. 1, pp. 159–166, 2010.

[11] R. Ancuti, I. Boldea, and D.-S. Andreescu, "Sensorless V/f control of high-speed surface permanent magnet synchronous motor drives with two novel stabilizing loops for fast dynamics and robustness", IET Electric Power Applications, Vol. 4, No. 3, pp. 149–157, 2010.

[12] S. Manabe, "Coefficient Diagram Method", 14th IFAC Symposium on Automatic Control in Aerospace, pp. 322-327, 1998.